Journal of Maps

ISSN: (Print) 1744-5647 (Online) Journal homepage: https://www.tandfonline.com/loi/tjom20

Shallow geophysics of the Asinara Island Marine Reserve Area (NW Sardinia, Italy)

Roberto Romeo, Luca Baradello, Rita Blanos, Pietro Paolo Congiatu, Diego Cotterle, Saul Ciriaco, Federica Donda, Michele Deponte, Vittorio Gazale, Emiliano Gordini, Emanuele Lodolo, Paolo Paganini, Alessandro Pavan, Carla Pietrapertosa, Paolo Sterzai, Giovanni Vargiu, Aldo Zanello, Riccardo Ramella & Daniel Gustavo Nieto Yabar

To cite this article: Roberto Romeo, Luca Baradello, Rita Blanos, Pietro Paolo Congiatu, Diego Cotterle, Saul Ciriaco, Federica Donda, Michele Deponte, Vittorio Gazale, Emiliano Gordini, Emanuele Lodolo, Paolo Paganini, Alessandro Pavan, Carla Pietrapertosa, Paolo Sterzai, Giovanni Vargiu, Aldo Zanello, Riccardo Ramella & Daniel Gustavo Nieto Yabar (2019) Shallow geophysics of the Asinara Island Marine Reserve Area (NW Sardinia, Italy), Journal of Maps, 15:2, 759-772, DOI: 10.1080/17445647.2019.1669498

To link to this article: https://doi.org/10.1080/17445647.2019.1669498

JOURNAL OF MAPS
2019, VOL. 15, NO. 2, 759–772
https://doi.org/10.1080/17445647.2019.1669498

Taylor & Francis
Taylor & Francis Group

Science

OPEN ACCESS Check for updates

Shallow geophysics of the Asinara Island Marine Reserve Area (NW Sardinia, Italy)

Roberto Romeo [a], Luca Baradello [a], Rita Blanos[a], Pietro Paolo Congiatu[c], Diego Cotterle[a], Saul Ciriaco[b], Federica Donda [a], Michele Deponte[a], Vittorio Gazale[c], Emiliano Gordini[a], Emanuele Lodolo [a], Paolo Paganini [a], Alessandro Pavan[a], Carla Pietrapertosa[d], Paolo Sterzai[a], Giovanni Vargiu[c], Aldo Zanello[c], Riccardo Ramella[a] and Daniel Gustavo Nieto Yabar[a]

[a]Istituto Nazionale di Oceanografia e di Geofisica Sperimentale (OGS), Trieste, Italy; [b]Shoreline Soc. Coop., AREA Science Park, Padriciano, Italy; [c]Parco Nazionale dell'Asinara – Area Marina Protetta 'Isola dell'Asinara', Porto Torres, Italy; [d]Istituto di Metodologie per l'Analisi Ambientale, Consiglio Nazionale delle Ricerche, Rome, Italy

ABSTRACT

We present a high-resolution swath bathymetric and backscatter map of the entire sector of the Marine Reserve Area (MRA) of the Asinara Island, along with a geological and sediment thickness map derived from the interpretation of a large set of high-resolution seismic profiles, and an airborne-derived hyperspectral image of the Asinara Island. Acquired data show that most of the eastern marine sector of the Asinara Island is characterized by quite gentle bathymetric gradients, whereas the western coastline appears to be very indented, with an articulated and rough morphology of the seafloor, which deepens sharply towards the open sea. The maps presented in this study at the 1:50.000 scale do not only provide the first, high-resolution bathymetry of the MRA of the Asinara Island but also may furnish the base for the creation of a benthic habitat map and a more comprehensive maritime spatial planning of this protected area.

ARTICLE HISTORY
Received 14 March 2019
Revised 11 September 2019
Accepted 16 September 2019

KEYWORDS
Multibeam bathymetry; high-resolution seismic; aerial hyperspectral survey

1. Introduction

The sea surrounding the Asinara Island (Figure 1), located at the NW corner of Sardinia (Italy) and separated by the main island by a narrow strait, was declared a Marine Reserve Area in 2002. It occupies an area of 10,732 ha and is divided into various environmental units according to their particular uniqueness and peculiarity. The Istituto Nazionale di Oceanografia e di Geofisica Sperimentale (OGS) of Trieste was committed by the Asinara Island National Park to conduct a series of geophysical surveys both offshore and onshore, along with specific seafloor samplings and biological-oriented investigations in the area of the Asinara Island. All of these studies had the common purpose to evaluate the possible impact of human-induced activities on the marine protected area, and eventually, reveal indications of illegal fishing activities. The surveys led to the collection of Multibeam bathymetric data, Side Scan Sonar images, single-channel high-resolution seismic reflection profiles (Chirp and Boomer seismic sources), bathymetry retrieval from Hyperspectral Remote Sensing Data, sediment samplings and seafloor photographs all around the Asinara Island from the coastal area down to *ca.* 110 m water depths. A specific objective of the offshore biological-oriented activities was to monitor the present-day distribution of the *Posidonia oceanica*, the most important endemic seagrass species of the Mediterranean Sea. It can form meadows or beds, which provide habitat for a large fauna community, thus increasing biodiversity of the coastal zone (Hemminga & Duarte, 2000; Gobert, Kyramarios, Lepoint, Pergent-Martini, & Bouquegneau, 2003). Because of the *P. oceanica* sensibility to specific environmental changes, its presence and abundance can be considered as an indicator of the overall quality of the coastal zone (e.g. Romero, Martìnez-Crego, Alcoverro, & Pérez, 2007; Ruiz & Romero, 2003). In this paper, however, we do not present the results obtained from biological analyses, as these aspects will be dealt with in another specific article.

Here we present three main maps derived from the analysis of the whole acquired geophysical dataset both offshore and onshore, as follows: (1) an airborne hyperspectral image of the Asinara Island; (2) a high-resolution seafloor bathymetric map covering the whole Asinara Marine Reserve Area, from the shoreline to about 110 m water depth; (3) an integrated subsoil geological map of the Asinara Marine Reserve Area.

2. Geological setting

The geology of the Asinara Island is dominated by the widespread outcrop of the Hercynian basement, which

CONTACT Roberto Romeo rromeo@inogs.it

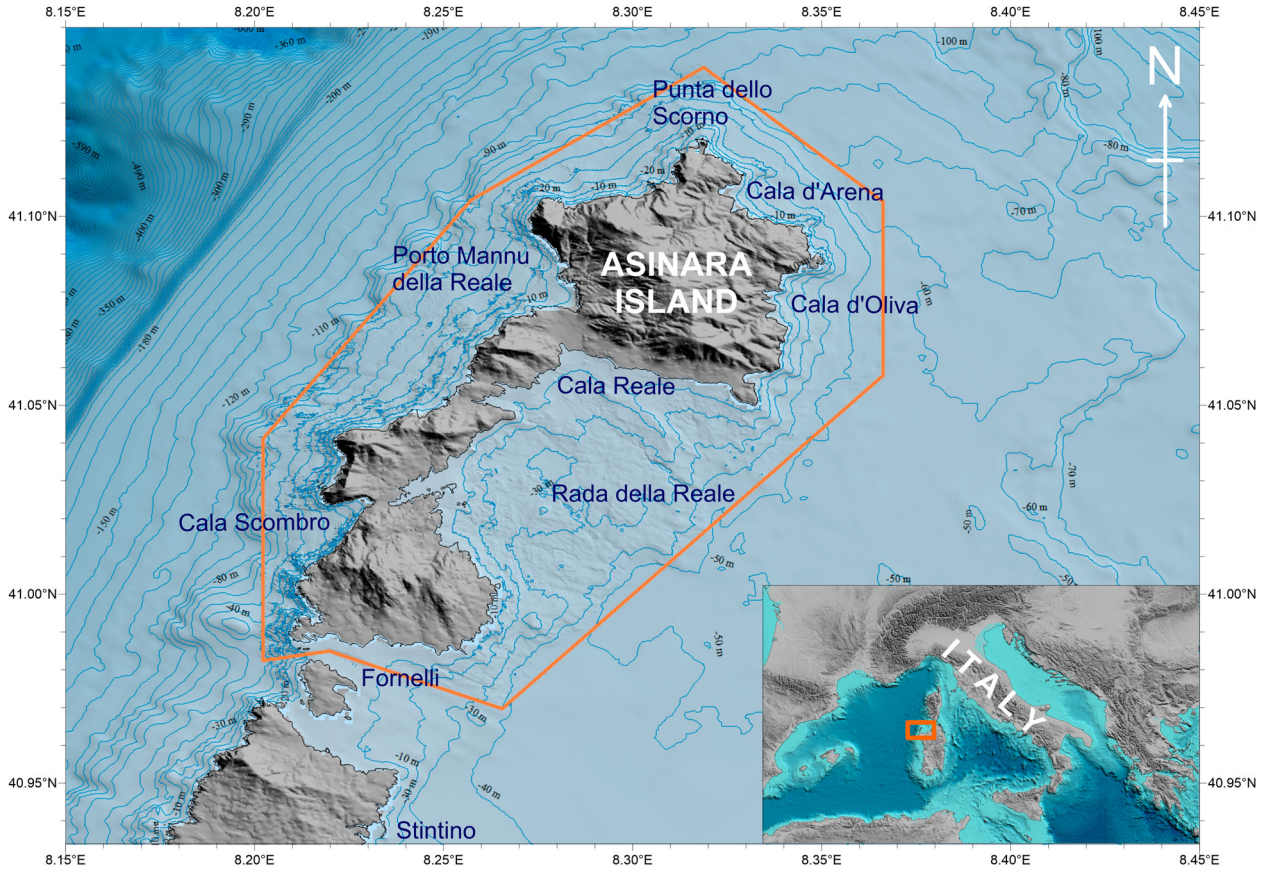

Figure 1. Location map of Asinara Island, northwest Sardinia (Italy). The orange line is the external perimeter of the Marine Reserve Area covered by the geophysical surveys. Data outside the orange perimeter have been taken from the EMODnet portal (http://www.emodnet-bathymetry.eu/) (Geographic coordinate system). The orange box in the lower right map indicates the location of the study area.

represents a segment of the South European Variscan belt (Cappelli et al., 1992; Carmignani et al., 1994; Matte, 1986). It includes the Corsica-Sardinia massif, which constitutes a microplate drifted away from Europe in the Oligocene (Alvarez, Cocozza, & Wezel, 1974). In Sardinia, the Variscan belt comprises three main tectonic domains: (1) a foreland belt consisting of Upper Cambrian-Lower Carboniferous sedimentary sequence; (2) a SW-verging stack of piled nappes formed by Paleozoic volcano-sedimentary sequences affected by thrusts and folds; (3) an inner zone, characterized by medium- to high-grade metamorphic rocks, and consisting of two different metamorphic complexes separated by the Posada-Asinara Line (Carmignani et al., 2001; Carmignani, Oggiano, Funedda, Conti, & Pasci, 2016; Carosi, Di Pisa, Iacopini, Montomoli, & Oggiano, 2004; Cuccuru, Casini, Oggiano, & Simula, 2018; Frassi, 2015). This tectonic lineament is a km-thick mylonitic belt (Cappelli et al., 1992; Elter, Musumeci, & Pertusati, 1990), which would be part of the South Hercynian Suture Zone between the Armorica and Gondwana continental margins (Cappelli et al., 1992). Studies have shown that it is a dextral tectonic transform that was active since the Precambrian and persisted during the Tertiary (Elter et al., 1990; Oggiano & Di Pisa, 1992; Pasci, 1997).

The Sardinia Island depositional environment has been characterized by repetitive marine transgressive and regressive episodes since the Triassic, which led to the formation of paleo-fluvial valleys known as 'rias', eroded during sea-level fall and low stand, and submerged during subsequent transgressions (Carmignani et al., 2001). Rias occur also along the eastern coast of the Asinara Island. During the Quaternary, a phase of general subsidence allowed the deposition of a marine to continental sedimentary succession, mostly consisting of marine and aeolian sandstones, together with fluvial conglomerates and gravel sands (Andreucci, Pascucci, & Clemmensen, 2006 and reference therein). The Holocene is dominated by alluvial plain sandy-gravel deposits, by aeolian sand by clayey lagoonal and coastal pond deposits (Carmignani et al., 2001). Along the western coast of Asinara Island, remnants of Tyrrhenian palaeo-beaches are also recognizable in places.

3. Methods

3.1. Multibeam sonar data acquisition and processing

The bathymetric survey was carried out in October 2015 and September 2016 using a portable, high-resolution Multibeam echosounder Teledyne Reson Seabat 7125. An area of 92 km^2 was mapped, covering about 90% of the total extension of the Asinara Marine Protected

Area. The transducer was mounted to a vertical pole integrally fixed with the boat hull. The Reson Seabat 7125 operates with a dual-frequency of 200–400 KHz, and is composed of 512 beams in equidistance or equiangular mode. The maximum ping rate is 50 Hz in very shallow water, while the swath coverage varies according to the water depth. To ensure the best data coverage, every single swath was superimposed to the adjacent one for about a third. To correct the data for the vessel's movements in terms of pitch, roll, yaw and heave, the inertial system Phins IXSEA and the motion reference unit TSS Mahrs were used. The Trimble dual-frequency DGPS DSM232 was the positioning system used for the entire survey, and the sound velocity profiles used to calibrate the Multibeam data were acquired with the Valeport SVP probe, deployed every day of acquisition at the beginning of the sea operations. All the equipment was installed on board of a 12.5 m long ship suitable for this kind of survey. The bathymetric data were acquired and processed with the Teledyne Reson PDS2000 software that provides, during acquisition, some automatic tools to detect and delete bad quality data. Acquired data were processed with the following sequence: (1) sensor calibration and geometry validation; (2) sound velocity profiles control; (3) positioning and tidal control; (4) application of statistic, slope, flying object and beam quality automatic filters; (5) data replay, with different points of view, to detect spikes and anomalies. Finally, a Digital Terrain Model (DTM), with a square cell from 1 to 10 m, was created. Tidal data used to correct the depth values were retrieved from the Porto Torres station of the 'National Tidegauge Network', managed by ISPRA (http://www.mareografico.it). Occasional bad sea and weather conditions during the two survey have made operations difficult, and in some cases introduced significant noise in the acquired data which imposed robust filtering to minimize steps in adjacent swaths. Multibeam data have been integrated with bathymetric data available from the EMODNET portal (http://portal.emodnet-bathymetry.eu) to cover areas outside the perimeter of the marine protected area and to produce the general map in Figure 2. In addition, in the areas close to the shoreline and in the jagged coastal areas with the presence of outcropping rocks, unattainable with the boat, the Multibeam map was complemented with airborne-derived hyperspectral measurements, as described in the next paragraphs.

3.2. High-resolution seismic data acquisition and processing

A high-resolution, single-channel seismic survey was realized in September 2015, which covered the entire area of the Asinara Marine Reserve Area: 104 seismic lines were acquired, for a total length of 284 km (Figure 3).

This survey complemented previous geophysical cruises performed by OGS in 2000 off northwestern Sardinia, in the frame of a project aimed at monitoring the water quality on the basis of the distribution of the seagrass *P. oceanica* (Donda et al., 2008). These former data, comprising CHIRP and Side Scan Sonar profiles, have been used in the frame of the present study to integrate the 2015 dataset. The specific purpose of the latter survey was appropriately cross all the geomorphological features recognized from the Multibeam data and to determine the thickness of the sediments that cover the bedrock. The Boomer seismic source used was a UWAK electrodynamic plate of Nordik Nord mounted on a catamaran and suspended at a depth of 40 cm beneath the sea-level. The plate is powered by a group of PULSAR 2002 capacitors connected to a 3.5 kW generator. The pulse generated by UWAK is a broad-spectrum impulsive type (400–6000 Hz with a dominant frequency of 2000 Hz) and leads to a sub-metric resolution. The receiving system was a single-channel GeoSense Streamer composed of 8 pre-amplified hydrophones connected in series and distributed over an active section of 3 m. This single-channel streamer achieves a strong increase in the signal-to-noise ratio by adding in phase the coherent signals (reflections coming from the sediments) and reducing the random noise. The acquisition system was a TRITON-ELICS acquisition card (24 bits A/D convert) installed on a PC, in a Windows environment and managed by the TRITON SBP-Logger software. The SBP-Logger software allows performing quality control in real time and simultaneously records data on hard disks in SEGY-IBM format. A DGPS AgGPS123-Trimble interfaced with the acquisition has guaranteed the positioning of the collected tracks. The PDS2000 navigation system (Teledyne Reson) was used to follow the planned routes. The acquisition geometry adopted during the survey was a parallel source-receiver. It is preferred to use this scheme with respect to the classic source-receiver in line since the water depth of several bays is less than the length of the streamer (Baradello & Carcione, 2008). The sampling rate was 0.05 ms, shot frequency 3 shot/s and record length 120–200 ms, acquiring the data with an average ship speed of four knots. The maximum acoustic penetration was about 80 m below seafloor with an approximately 0.2 m of vertical resolution. The seismic data were processed with the Focus software (PARADIGM) on a Linux workstation. Primarily, the respective coordinates were merged and associated to every trace in UTM 32 WGS84. The relative offset source-receiver (3 m) was also inserted in the headers and then the Normal Move Out correction was applied to bring back the profiles at the zero-offset condition. No tidal corrections have been applied to the profiles. To eliminate electrical disturbances and noise introduced by frequent bad sea conditions (phenomenon of ripple in the seismic signal), algorithms have

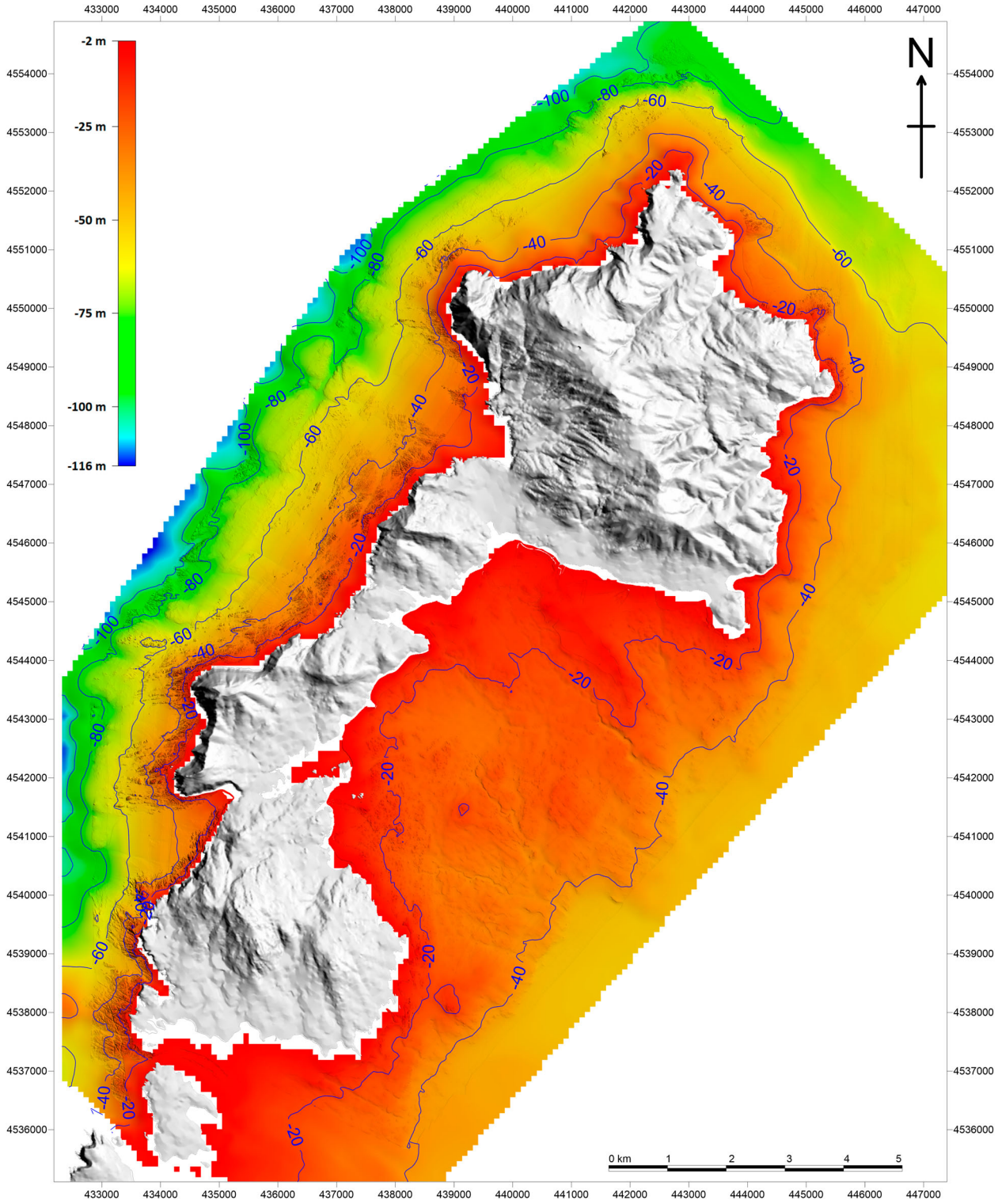

Figure 2. High-resolution swath bathymetric map of the Asinara Marine Protected Area, produced by merging Multibeam, airborne-derived hyperspectral methodologies, and EMODnet data. The digital terrain model of the Asinara Island has been taken from http://www.sardegnageoportale.it

been applied by averaging the amplitudes and frequencies on temporal windows of groups of adjacent traces and then attenuating them (static correction). The spherical divergence has been applied on the data, starting from the seafloor, and an Automatic Gain Control (10–20 ms windows). Further band-pass filters were applied according to the spectral characteristics of the individual profiles. The result of the interpretation of the acquired seismic profiles is a sediment thickness map (isopach map in two-way traveltime, TWT), produced by subtracting the depth of the seafloor from the base of the marine sediments (Figure 4). The isopach map was realized with the Surfer software, using the Kriging method with a gridding lattice of 50 m. Because the absence of direct sound speed measurements for the shallowest sedimentary strata, the depth conversion of

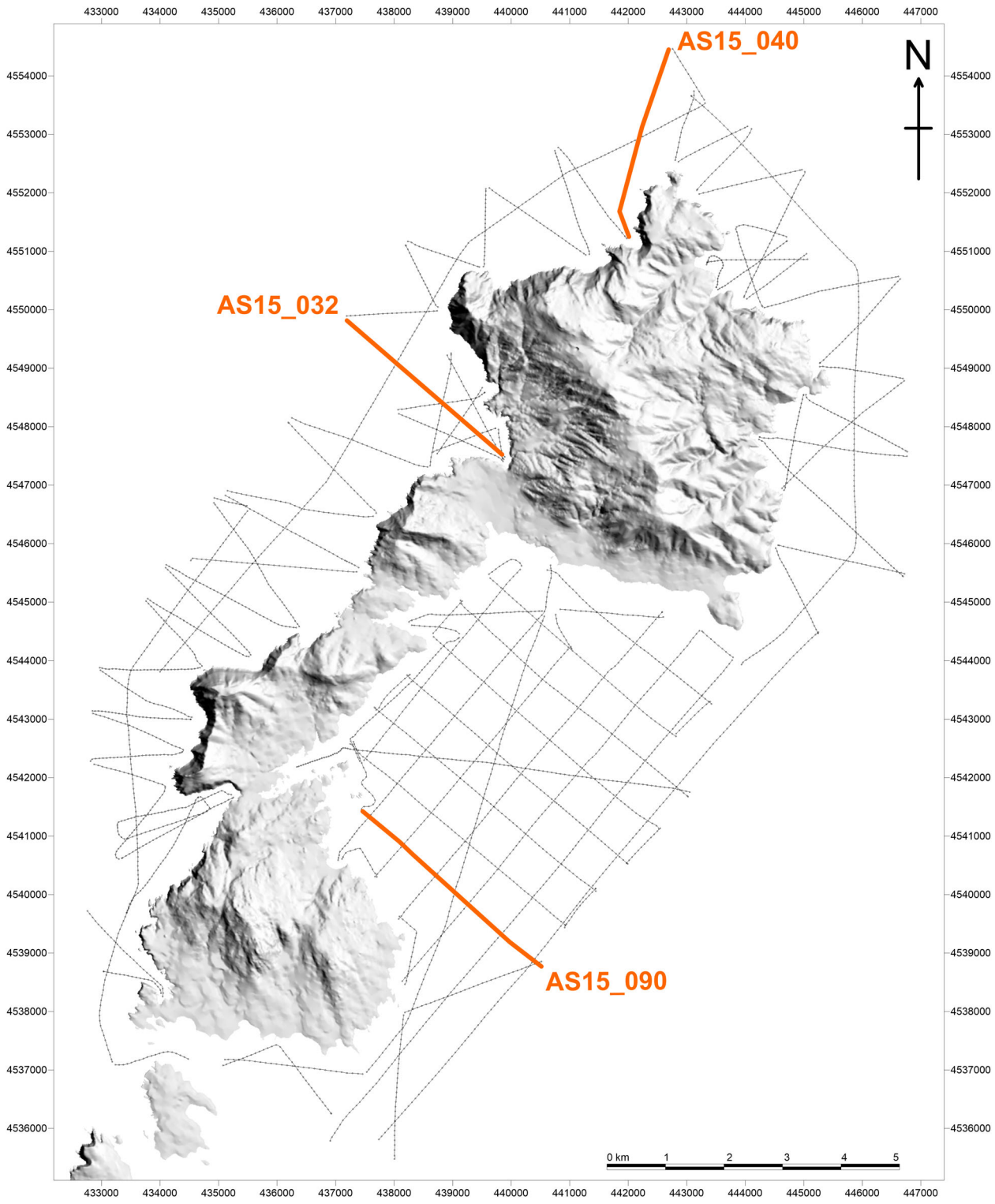

Figure 3. Position map of the high-resolution seismic profiles acquired in 2015.

the profiles was made by applying an average value of 1650 m/s, as proposed in the literature for wet sands and silt (Anderson, 1974).

3.3. Side Scan Sonar survey

The Side Scan Sonar (SSS) was towed astern of the boat and emits directional acoustic waves downwards and sideways. The instrument used in the 2015 and 2016 surveys is an Edgetech DF1000, with a frequency of 100 and 500 kHz, a pulse length of 0.1 and 0.01 ms and a swath of 200–320 m. A fixed layback was used for this survey. The measurements were performed mainly along parallel transects, whose distance was defined as a function of depth to ensure an overlap greater than 60%.

The data acquired during the survey were subjected to quality control and preliminary processing directly in the field in order to ascertain the quality of the collected data and verify the coverage of the area. The acquired data were processed using the Coda Octopus

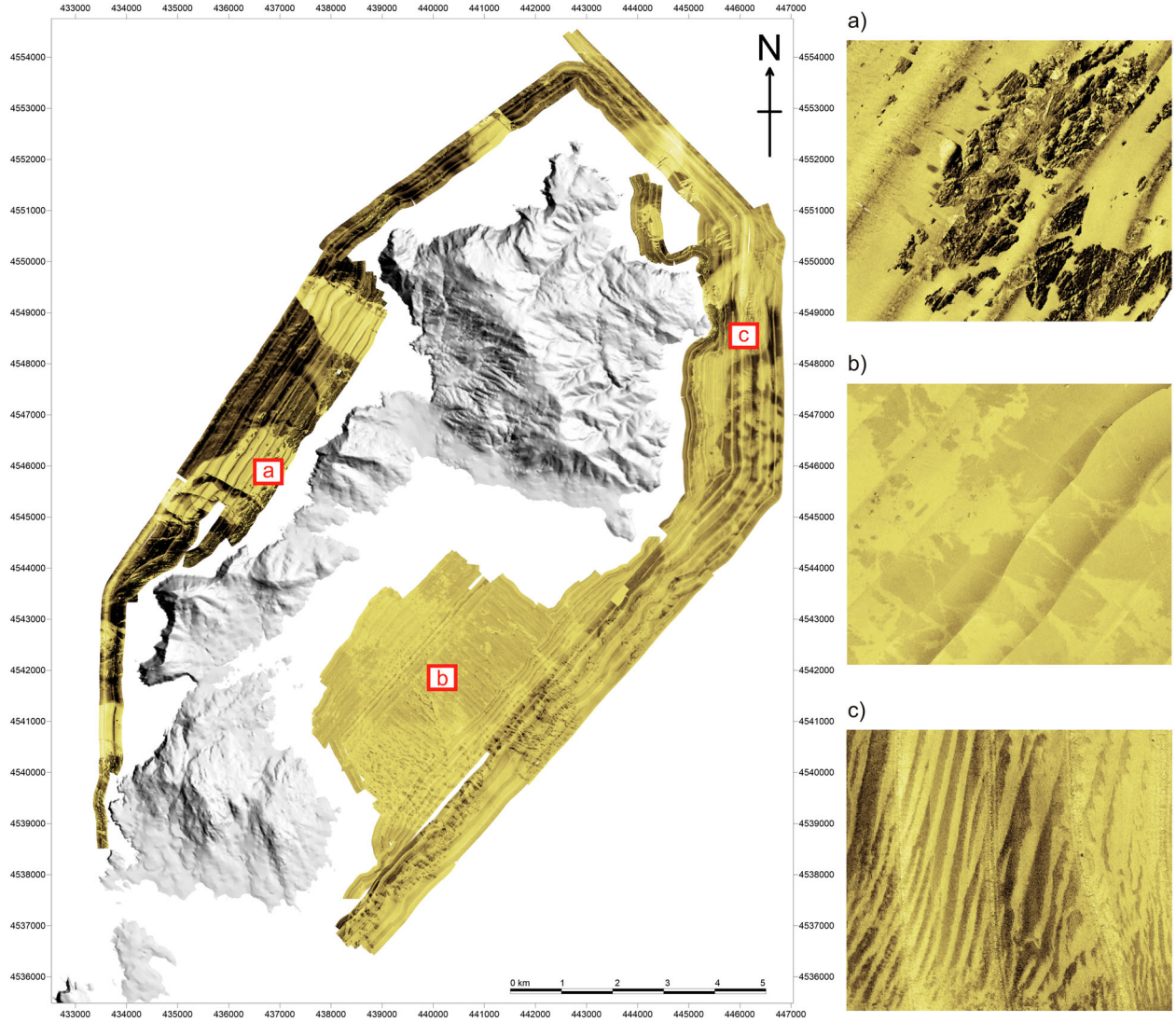

Figure 4. Backscatter mosaic map of the Asinara Marine Protected Area, produced by merging Side Scan Sonar data. (a) rock outcrops (b) fine sediments and *P. oceanica* meadows (c) alternating fine and coarse sandy seafloor. See text for details.

Geokit Mosaics software and graphically represented in a mosaic in order to identify any objects on the seafloor and define its morphological characteristics.

The backscattered recorded energy provide different types of information about the nature of the point imaged. The backscattering from the seafloor is influenced by three factors: local geometry of ensonification, the roughness of the surface and intrinsic properties of the seafloor. The SSS survey allowed us to observe natural seabed features, aids in identifying subsurface geological features and man-made features. The interpretation of backscatter intensity images has allowed us to identify areas of fine or coarse sediments, seabed topography and relief, bedforms, rock outcrops and boulders, seabed channels, *P. oceanica* meadow and scours. The scours are connected with illegal trawl fisheries, with a significant impact on marine benthic habitats.

3.4. Aerial hyperspectral survey

On 28 October 2016, an aerial hyperspectral survey was carried out on the entire Asinara Island and on the Island of Piana for a total data coverage of *ca.* 120 km^2 (Figure 5).

As well known, the main objective of hyperspectral imaging is to obtain the spectrum for each pixel in the image of a scene, with the purpose of finding objects, identifying materials, or detecting processes (e.g. Chang, 2003; Grahn & Geladi, 2007). This method has several applications in different fields; it can be used, for example, in environmental studies to identify oil spill, pollution or CO_2 emissions, as well as in agricultural sciences to characterize biophysical properties, disease and stress of vegetation.

Hyperspectral sensors acquire images in narrow and continuous parts of the electromagnetic spectrum. Each image is composed of pixels and each pixel contains a continuous spectrum that can be used to identify, with high precision, different type of materials. These 'fingerprints' are used to identify the materials that make up a scanned object. The hyperspectral methodology was used to cover not only the emerged part of the island but also the shallow areas adjacent to the coastline which were not surveyed by the Multibeam because

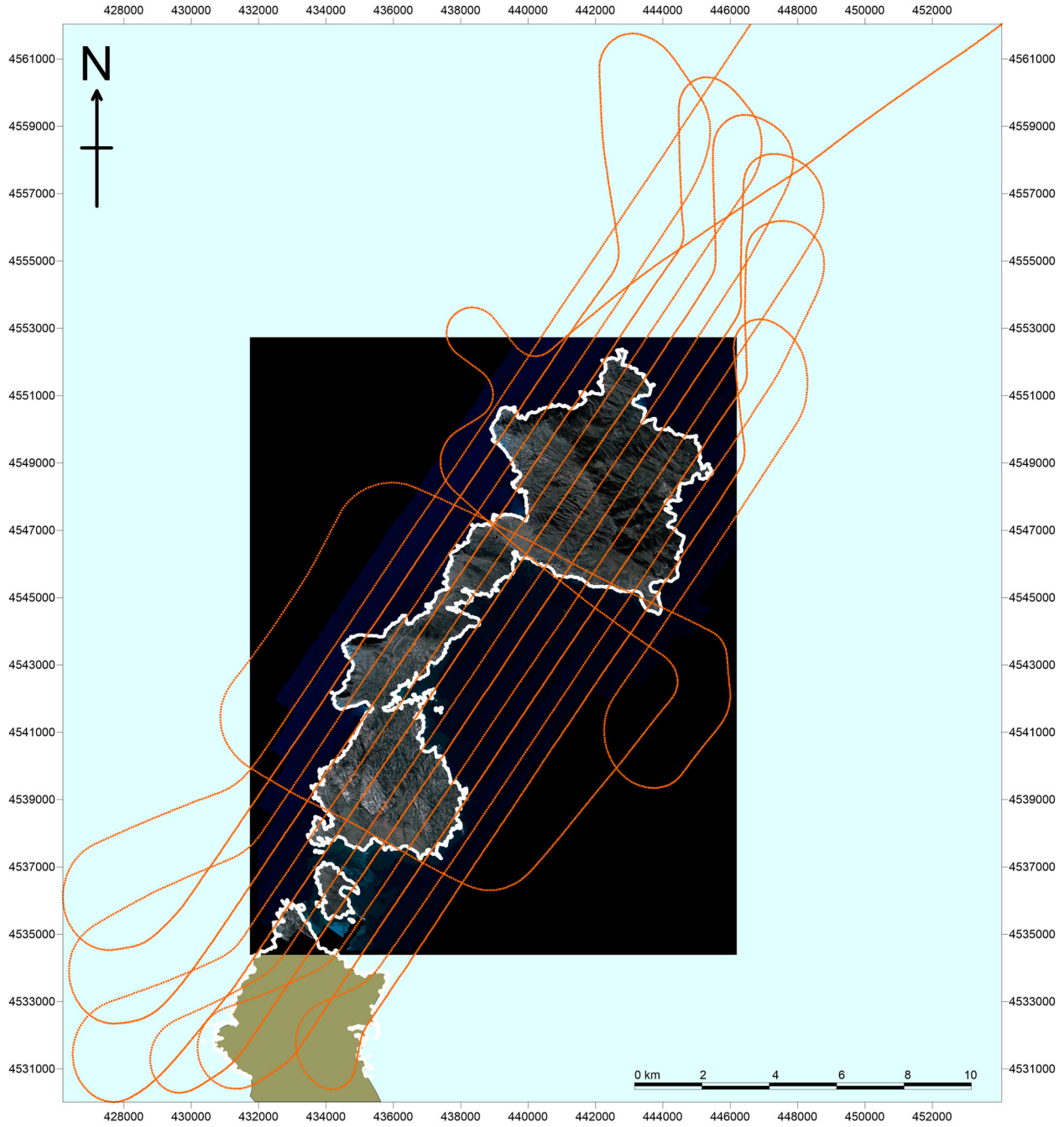

Figure 5. Fly-tracks of the airborne hyperspectral survey.

physical limits (rocky outcrops, very shallow water, etc.) which prevented a safe navigation. The acquisition system, installed on a Partenavia P68 aircraft, consisted of a hyperspectral camera and an inertial unit rigidly fixed to the fuselage of the aircraft, using an aluminum plate. In this way, the relative movements between sensor and inertial unit were reduced to the minimum. The system was connected to a GPS/INS (Inertial Navigation System) sensor which provides reliable, continuous position, velocity and altitude. Within the spectral range of 400–970 nm, corresponding to the near visible-infrared interval, it is possible to configure the acquisition of up to a maximum of 252 bands, with variable bandwidth. The following parameters were considered during the acquisition: (1) overlapping of the strips not less than 35% in the transverse direction; (2) resolution of the acquired images (intended as a pixel ground dimension) not exceeding 1 m; (3) acquisition of 61 bands in the spectral range of 400–970 nm with an average spectral resolution of 9.46 nm. Table 1 summarizes the most important parameters of the survey.

The flight has been planned during the ideal weather conditions (clear sky, no fog, weak wind, calm sea) to

Table 1. Parameters of the survey.

Flight height	1700 m
Aircraft speed	120 kts
Distance between flight lines	700 m
Total survey length	180 km
Total survey time	2 h
Resolution (ground pixel size)	1 m

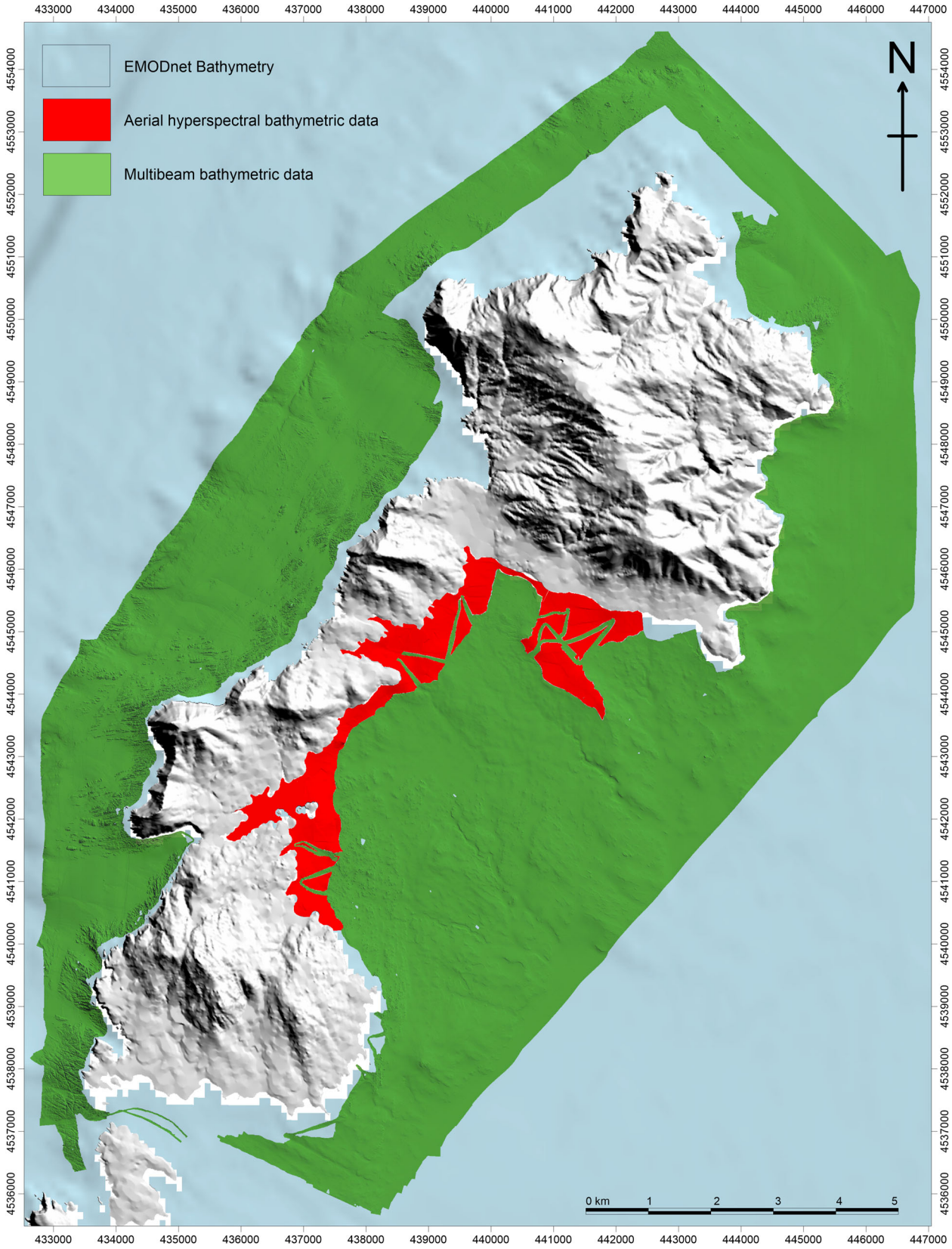

Figure 6. Coverage of the Multibeam bathymetric data (green), bathymetric hyperspectral data (red), EMODnet bathymetric data (light blue) superimposed on the topographic datum of the island (shaded relief).

ensure good quality of the acquired data and maximum visibility of the seafloor in shallow water areas. The acquired data were radiometrically and geometrically corrected. Radiometric correction removes the dark current signal (acquired with closed shutter) and converts Digital Number (DN) to radiance. Geometric correction removes geometric distortions from imagery and transform image data to real-world map coordinates. In literature there is a variety of methodologies to obtain the bathymetry from multispectral data, especially in

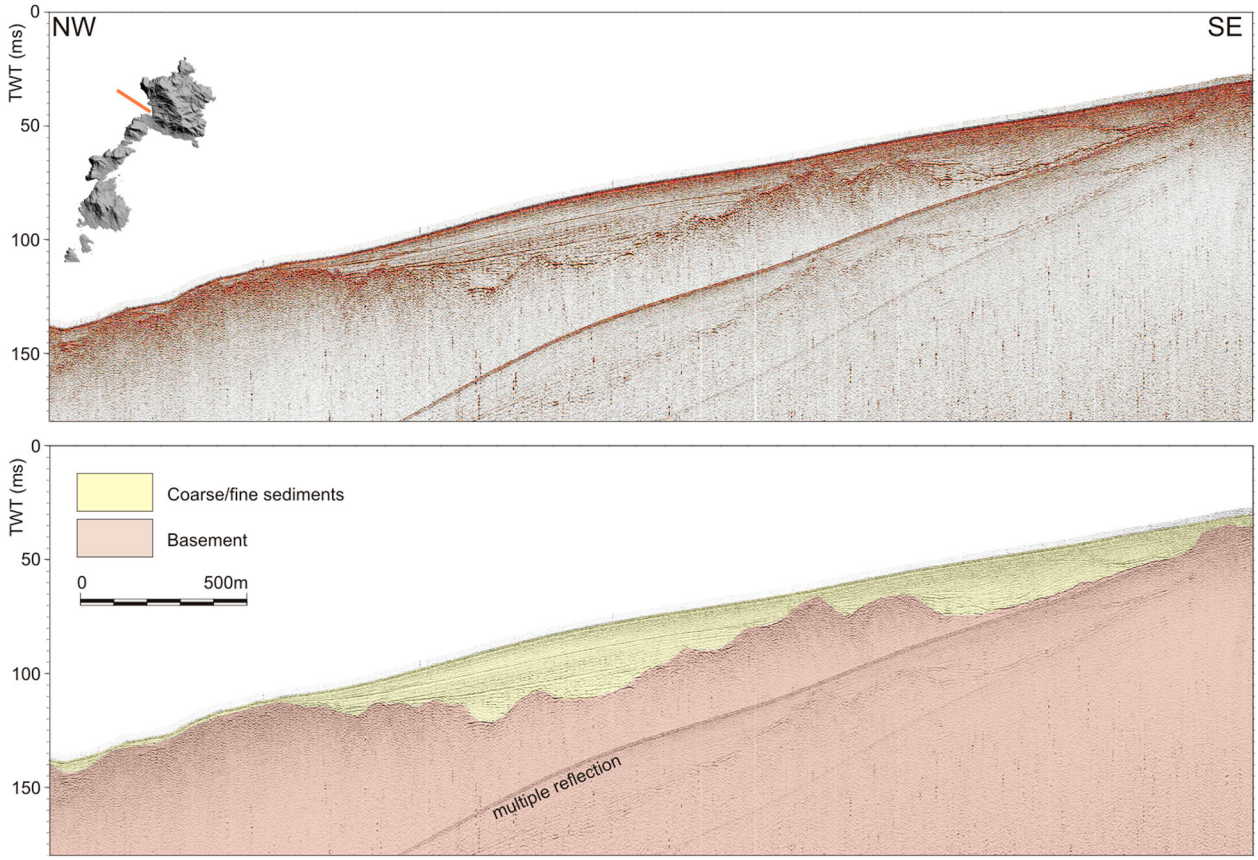

Figure 7. Un-interpreted (above) and interpreted (below) seismic profile AS15_032 acquired within the cove of Porto Mannu della Reale, where ca. 27 m thick deposits have been recorded. The top of the basement, characterized by an acoustically opaque signal, is clearly recognizable at the base of thinly stratified deposits which onlap it.

areas characterized by clear waters (i.e. the Caribbean Sea), that allows a minimal absorption of the electromagnetic signal in the visible interval, especially in the spectral portion of green and blue, while red is absorbed in the first centimeters. There are a series of empirical formulas that have been proposed, although these are very difficult to apply due to the complexity of modeling the behavior of the electromagnetic signal in a variable environment as the sea water. In order to calculate the water depths, we applied the following equation to derive the bathymetry, using multiple bands, according to the formula proposed by Hamilton, Davis, Rhea, Pilorz, and Kendall (1993):

$$\text{Depth}\,(Z) = a0 + a1(\text{Rrs}(\lambda 1)) + a2(Rrs(\lambda 2)). \quad (1)$$

In this formula, Rrs is the reflectance at a particular wavelength, while $a0$, $a1$ and $a2$ are linear coefficients. To determine these coefficients, the acquired bands were analyzed taking into consideration the superficial spectra in the transition zones with deeper waters. Two wavelengths characterized by low background noise and maximum penetrability were chosen, $||\lambda 1 = 460$ nm and $||\lambda 2 = 560$ nm. By applying a multiple regression to the data according to Equation (1), the coefficients $a0 = 32$, $a1 = 21$ and $a2 = 39$ were calculated with a correlation coefficient equal to 0.96. Despite the good statistical results, the comparison between Multibeam data and hyperspectral-derived bathymetry did not give fully satisfactory results. The Equation (1), among other parameters, would require a 'homogeneous turbidity' of the water in order to apply the linear relation. Unfortunately, this condition did not occur and therefore Equation (1) can only be applied locally. Due to some altimetric shifts, it was not possible to perform direct data integration among Multibeam and hyperspectral-derived bathymetry. Therefore it was preferred to apply a merging by making a fit to the least squares with bilinear functions taking Multibeam data as ground truth and integrating with the bathymetry deriving from the hyperspectral in the areas not covered by Multibeam data. The data were subsequently filtered with anisotropic filters in order to homogenize the texturing of the data. Data merging was performed using some modules of the GRAVSOFT software using the programs GEOIP (data gridding by least squares collocation) and GCOMB (data merging with different data spacing) (Forsberg, Tscherning, & Knudsen, 2003). After data integration, a filtering operation was required, as the two data had different spatial resolution. Therefore, it was necessary to filter the data in order to harmonize it. After an analysis of various filters used to enhance quality of images, the best result was achieved applying an anisotropic filter (Martin-Fernandez, Munoz-Moreno, & Alberola-

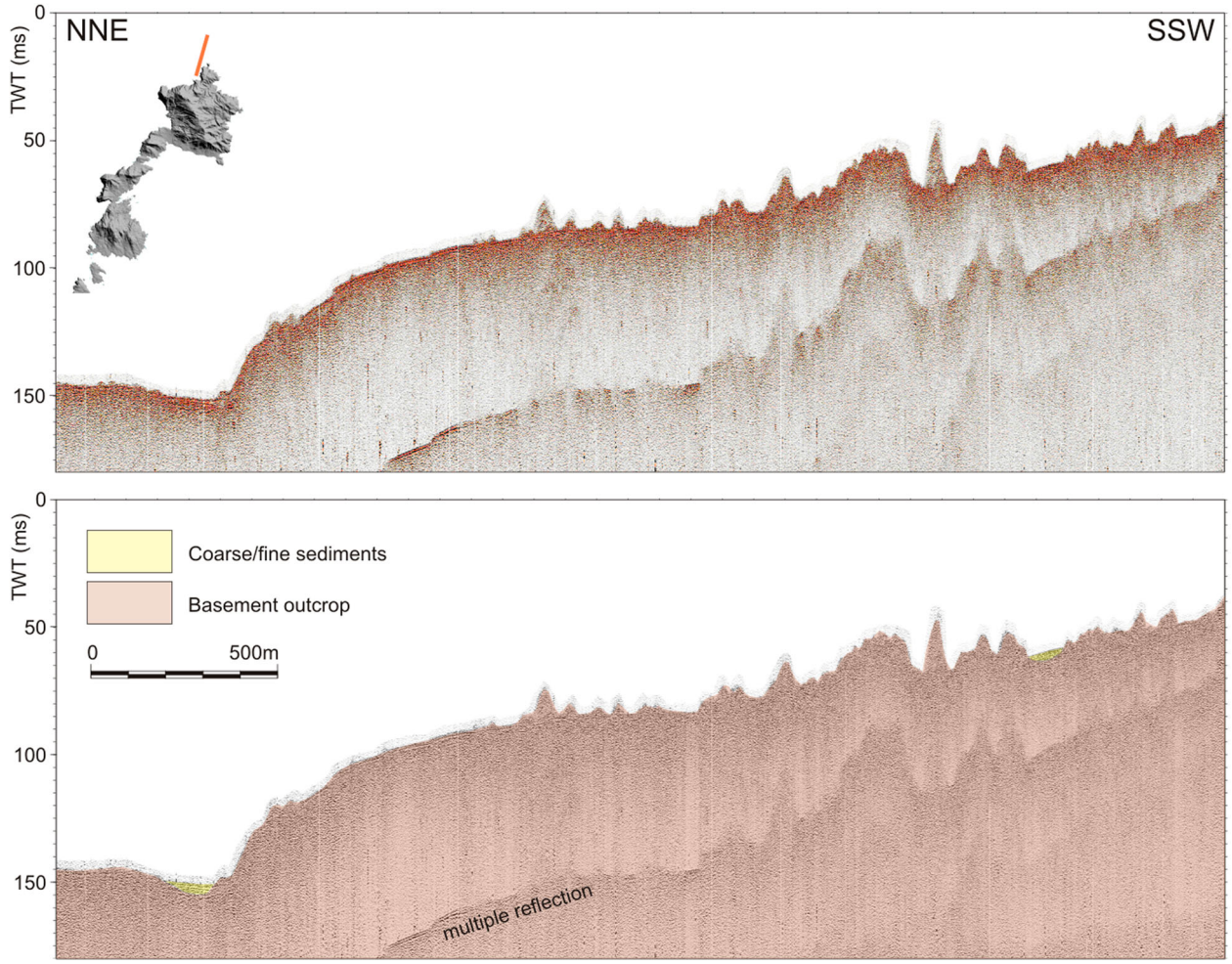

Figure 8. Un-interpreted (above) and interpreted (below) seismic profile AS15_040 acquired in the northern sector of the study area, where the basement is widely outcropping and characterized by rough, sediment-starved reliefs up to 15 m high.

Lopez, 2006). The final result is reported in Figure 6. The Cala Reale area proved to be particularly suited for the integration of the Multibeam data with the hyperspectral-derived data, due to the clarity of the water and hence with good penetration of the hyperspectral signal. In other marine areas of the Asinara Island where water depths are more pronounced, as in the case of the western part of the island, the integration of the two methodologies was not possible.

4. Data interpretation

4.1. Multibeam map

The Multibeam map highlights the different morphologic characteristics of the western and eastern coastal areas of the Asinara Island. As already mentioned in previous studies (i.e. Donda et al., 2008), the eastern marine sector is characterized by quite gentle bathymetric gradients, whereas the western sector deepens sharply towards the open sea. Here, a very irregular seafloor morphology reflects the occurrence of widespread basement highs, which frequently outcrop in the northernmost tip of the study area (Figures 7–9), in the form of sediment-starved reliefs (see also Figure 8 of Donda et al., 2008). The eastern sector of the study area, especially within Rada della Reale, is characterized by the predominance of a relatively flat seafloor, except in its northern sector, where the basement outcrops. The high-resolution data allow identifying an NW–SE trend of these outcropping basement reliefs, which apparently align with the Posada-Asinara line.

4.2. Isopach map

The high-resolution seismic data allow to clearly discerning the occurrence of the sub- and outcropping basement, characterized by an acoustically opaque signal, from fine-to-coarse grained sediments. In the northern portion of the study area, the basement is widely outcropping and is constituted by rough, sediment-starved reliefs up to 15 m high. In the central and southern areas, commonly sediments deposited between the basement reliefs, characterized by a smoother morphology compared to the northern sector.

In particular, the seismic data highlighted the presence of one or more sedimentary sequences, characterized by different acoustic facies, which are delimited at both the base and the top by horizons with onlap and downlap terminations. The isopach map, like the case

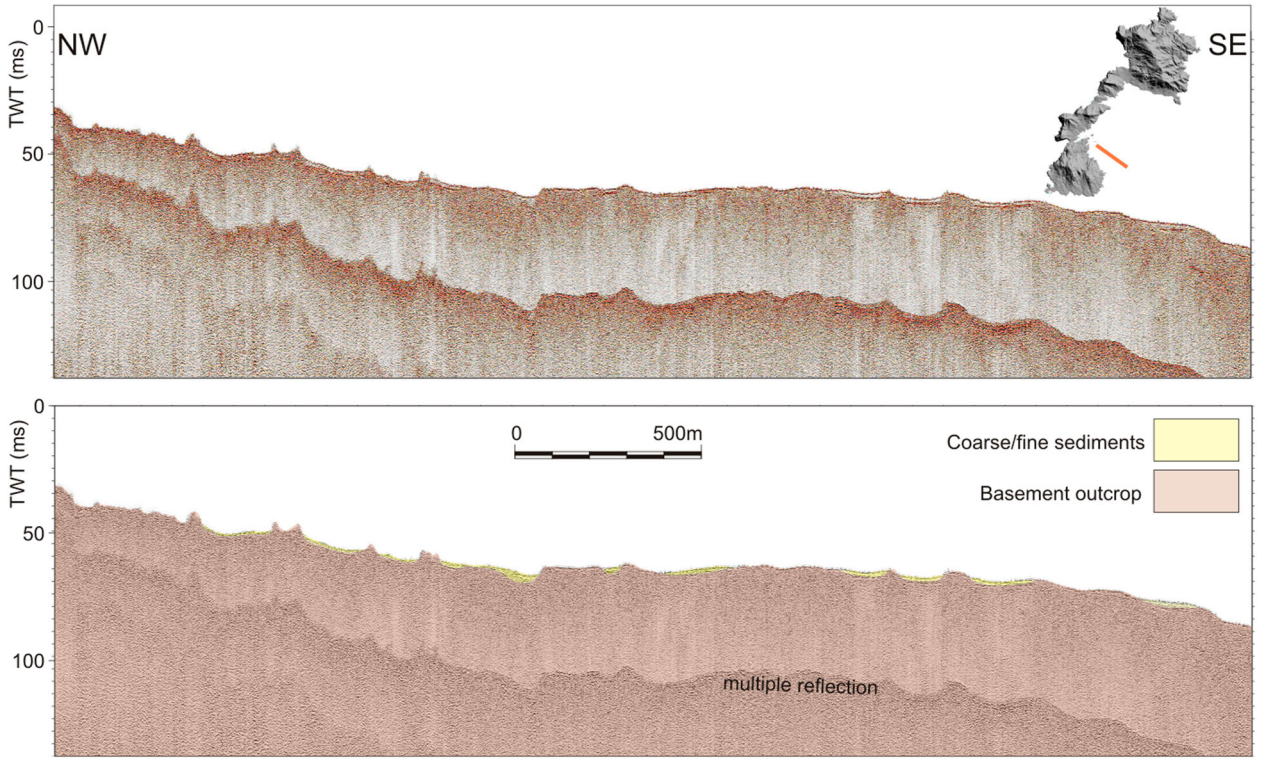

Figure 9. Un-interpreted (above) and interpreted (below) seismic profile AS15_090 acquired in the southern part of Rada della Reale. Here the seafloor appears to be interspersed with widespread basement outcrops, with a few-meters-thick sediments deposited between the basement reliefs.

of the swath bathymetric map, reveals the remarkable differences between the western and the eastern sector of the study area. Here, and in particular within Rada della Reale, the sediment thickness varies remarkably, and two distinct areas may be identified: in the southern part of Rada della Reale, the basement is largely outcropping, where the sediment cover is very thin (0.5–1 m); conversely, in the northern part of Rada della Reale, fine-to-coarse sediments are predominant.

The largest sedimentary deposits, both in extension and in thickness, were found in the west side of the island. The deposit of Cala Scombro di Fuori has a maximum thickness of about 17 m, with the occurrence of well layered sediment onlapping on the basement. The highest sediment thickness has been recorded on seismic profile AS15_032 in the cove of Porto Mannu della Reale, where the basement top, clearly recognizable at the base of thinly stratified deposits onlapping it, lies at a depth of 27 m (see Figures 7–9).

4.3. Backscatter mosaic

The backscatter Side Scan Sonar data were used, in conjunction with the Multibeam swath bathymetry to obtain a morphological description of the seafloor (Figure 10). Three main acoustical patterns, defined as types (a), (b) and (c) were identified and mapped (Figure 10).

Type (a) characterizes the outcrop of sediment-starved basement reliefs (Figure 10(a)). Along the northwestern coast of Asinara Island, from Punta Tumbarino to Porto Mannu, the seafloor is highly irregular, with rocky reliefs of various shapes and orientation, which stand out a few meters from the surrounding seabed consisting of coarse sands. These morphologies can also be observed inside the Rada della Reale, where the seafloor is constituted by an almost flat sandy surface interspersed with widespread basement outcrops. In this area, we also observe some channels that are emplaced between the basement reliefs within Rada della Reale, which display a roughly NNW–SSE trend.

Type (b) is constituted by fine-grained sediments, alternating with extensive *P. oceanica* meadows. It characterizes the seafloor of the inner part of Rada della Reale. This Type is related to the presence of *P. oceanica*, which occurs as broad beds within Rada della Reale, but also is present inside the Rada dei Fornelli. The seagrass can be associated with a sandy seafloor where round-shaped intermatte depressions are seen (Figure 10(b)). A progressive seaward reduction of the *P. oceanica* seagrass extension is clearly visible in the outer part of Rada della Reale. It is suggested that such holes in the meadows are mostly created by anthropic activities (i.e. anchors of boats). Along the western coast of Asinara Island, water currents can be particularly vigorous in the intermattes, leading to sediment resuspension and consequent inhibition of the growth of the *P. oceanica*.

Type (c) is represented by an alternating fine and coarse sand deposits. This acoustic Type is predominant along the northeastern coast of Asinara Island

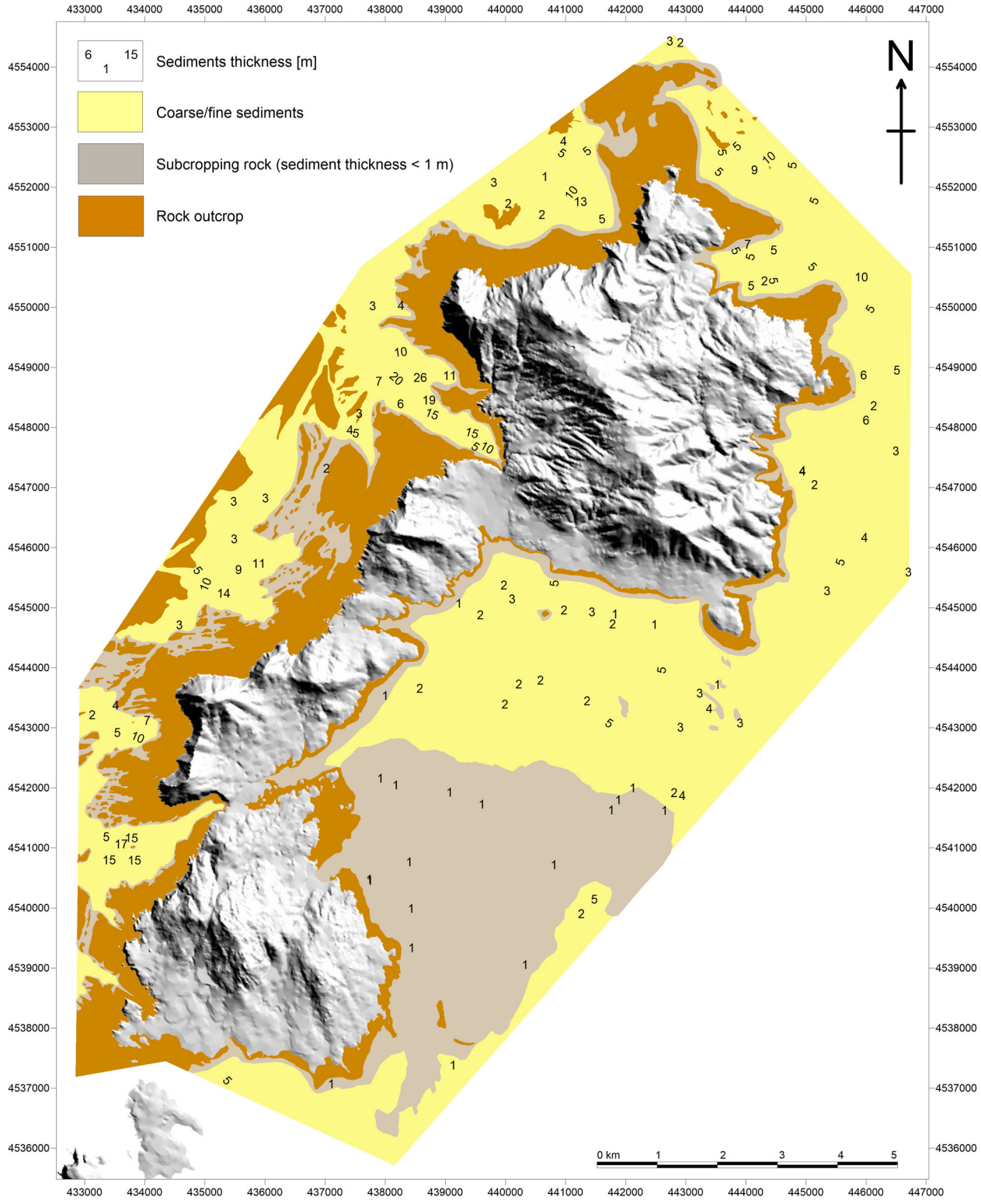

Figure 10. Distribution of seabed types and sediment thickness identified offshore the Asinara Island.

(Figure 10(c)) in water depths deeper than 30 m and in the range 40–50 m water depth as a rule, but it has also been identified in water depths shallower than 10 m. Along the northeastern side of Asinara Island, in front of Punta dei Corvi and Punta Sabina, patchy sand ribbons and dune fields are found between outcrops of the morphologically irregular basement. The sand ribbons have likely been formed by seaward-directed bottom currents along the sides of the rocky points that are exposed to large waves during westerly storms. Strong wave-generated orbital currents have been proposed as the cause of the medium to coarse sand dune fields identified along most of the western coast of Asinara Island.

5. Conclusions

High-resolution Multibeam and Side Scan Sonar data, single-channel high-resolution seismic reflection profiles, and airborne hyperspectral surveys collected

by OGS in the Asinara Island Marine Reserve Area have allowed to derive: (1) a detailed bathymetric map of the entire coastal area from the shoreline to 110 m water depths; (2) an isopach map of sediments deposited above the metamorphic basement; (3) an hyperspectral image of the Asinara Island along with an airborne-derived bathymetry of the near-to-the-coast areas which complemented the Multibeam data. Acquired data have shown that the western and eastern coastal areas of the Asinara Island are quite different from a morphologic point of view. The eastern sector, shallower than the wester sector, presents gentle bathymetric gradients, where the seafloor is characterized by the predominance of a fine-to-coarse sands. The western sector is characterized by a quite complex seafloor morphology, and bathymetric gradients are very pronounced. However, the sedimentary cover locally reaches significant thickness, especially within Cala Scombro di Fuori and Porto Mannu della Reale, where up to 27 m thick sediments occur. These maps may provide a reference base for further studies oriented to benthic habitat mapping, and, in general, for a more comprehensive maritime spatial planning of this marine protected area.

Software

The high-resolution seismic profiles were acquired with the SB-logger by Triton using Teledyne PDS200 for navigation and positioning. The seismic data were processed with Paradigm Focus and interpreted using Kingdom Seismic and Geological Interpretation Software IHS Markit. The isopach map was realized with the Golden Software Surfer. Bathymetric data were acquired and processed with Teledyne PDS2000, as well as the final DTM. The final mosaic was optimized with Global Mapper. The maps were produced using Esri ArcGIS.

The acquired data were processed using the Coda Octopus Geokit Mosaics software and graphically represented in a mosaic.

The hyperspectral data were acquired through the AISAEagle Airborne Hyperspectral System VNIR connected to GPS/Inertial Navigation System Span Novatel – iMAR FSAS. Inertial Explorer post-processing software from the NovAtel Waypoint Products Group was used to process GPS/INS data and define the trajectory and attitude (SBET) of the aircraft during the acquisition of hyperspectral data. The Digital Terrain Model obtained from lidar data was processed with the Terrasolid suite software (Terrascan and Terramodeler).

ENVI software was used to apply both radiometric calibration and georectification to the AISA images (CaliGeo software, a plug-in running under ENVI user interface) and to produce image mosaics.

The Hamilton et al. (1993) equation was used to obtain the bathymetry from radiometrically and geometrically corrected data.

GRAVSOFT (module GEOIP and GCOMB) was used to performe merging of hyperspectral and Multibeam data. The final maps were produced using Surfer and Esri ArcGIS.

Acknowledgements

We thank the crew of the fishing boat Sirius (master Balzano – fishermen cooperative Stintino) for the availability during the sea surveys.

Disclosure statement

No potential conflict of interest was reported by the authors.

ORCID

Roberto Romeo http://orcid.org/0000-0001-5867-8998
Luca Baradello http://orcid.org/0000-0002-9796-4521
Federica Donda http://orcid.org/0000-0002-1284-5866
Emanuele Lodolo http://orcid.org/0000-0002-4706-2095
Paolo Paganini http://orcid.org/0000-0002-5605-6164

References

Alvarez, W., Cocozza, T., & Wezel, F. C. (1974). Fragmentation of the Alpine orogenic belt by microplate dispersal. *Nature*, *248*, 309–314.

Anderson, R. S. (1974). Statistical correlation of physical properties and sound velocity in sediments. In L. Hampton (Ed.), *Physics of sound in marine sediments, marine science* (pp. 481–518). Boston, MA: Springer.

Andreucci, S., Pascucci, V., & Clemmensen, L. (2006). Upper Pleistocene coastal deposits of West Sardinia: A record of sea-level and climate change. *GeoActa*, *5*, 79–96.

Baradello, L., & Carcione, J. (2008). Optimal seismic-data acquisition in very shallow waters: Surveys in the Venice lagoon. *Geophysics*, *73*(6), 59–63. doi:10.1190/1.2976117

Cappelli, B., Carmignani, L., Castorina, F., Di Pisa, A., Oggiano, G., & Petrini, R. (1992). A Hercynian suture zone in Sardinia: Geological and geochemical evidence. *Geodinamica Acta*, *5*(1–2), 101–118.

Carmignani, L., Carosi, R., Di Pisa, A., Gattiglio, M., Musumeci, G., Oggiano, G., & Pertusati, P. C. (1994). The Hercynian chain in Sardinia (Italy). *Geodinamica Acta*, *7*, 31–47.

Carmignani, L., Oggiano, G., Barca, S., Conti, P., Salvatori, L., Eltrudis, A., … Pasci, S. (2001). *Note illustrative della Carta Geologica della Sardegna a scala 1:200.000. Memorie descrittive della Carta Geologica d'Italia: Geologia della Sardegna, 51*. Roma: Istituto Poligrafico e Zecca dello Stato.

Carmignani, L., Oggiano, G., Funedda, A., Conti, P., & Pasci, S. (2016). The geological map of Sardinia (Italy) at 1: 250,000 scale. *Journal of Maps*, *12*(5), 826–835.

Carosi, R., Di Pisa, A., Iacopini, D., Montomoli, C., & Oggiano, G. (2004). The structural evolution of the Asinara Island (NW Sardinia, Italy). *Geodinamica Acta*, *17*(5), 309–329.

Chang, C.-I. (2003). *Hyperspectral imaging: Techniques for spectral detection and classification*. New York: Springer Science & Business Media.

Cuccuru, S., Casini, L., Oggiano, G., & Simula, E. N. (2018). Structure of the Castellaccio Pluton (Asinara Island, Italy). *Journal of Maps*, *14*(2), 293–302.

Donda, F., Gordini, E., Rebesco, M., Pascucci, V., Fontolan, G., Lazzari, P., & Mosetti, R. (2008). Shallow water seafloor morphologies around Asinara Island. *Continental Shelf Research*, *28*, 2550–2564.

Elter, F. M., Musumeci, G., & Pertusati, P. C. (1990). Late Hercynian shear zones in Sardinia. *Bollettino della Società Geologica Italiana*, *114*, 147–154.

Frassi, C. (2015). Structure of the Variscan metamorphic complexes in the central transect of the Posada-Asinara Line (SW Gallura region, Northern Sardinia, Italy). *Journal of Maps*, *11*(1), 136–145.

Forsberg, R., Tscherning, C. C., & Knudsen, P. (2003). An overview manual for the GRAVSOFT geodetic gravity field modelling programs. *Kort og Matrikelstyrelsen*, Draft 1. Ed.

Gobert, S., Kyramarios, M., Lepoint, G., Pergent-Martini, C., & Bouquegneau, J. M. (2003). Variations at different spatial scales of Posidonia oceanica (L.) Delile beds; effects on the physico-chemical parameters of the sediment. *Oceanologica Acta*, 26, 199–207.

Grahn, H., & Geladi, P. (2007). *Techniques and applications of hyperspectral image analysis*. John Wiley & Sons. ISBN 978-0-470-01087-7.

Hamilton, M. K., Davis, C. O., Rhea, W. J., Pilorz, S. H., & Kendall, L. C. (1993). Estimating chlorophyll content and bathymetry of Lake Tahoe using AVIRS data. *Remote Sensing of Environment*, *44*, 217–230.

Hemminga, M. A., & Duarte, C. M. (2000). *Seagrass ecology*. Cambridge University Press.

Martin-Fernandez, M., Munoz-Moreno, E., & Alberola-Lopez, C. (2006). A speckle removal filter based on an anisotropic wiener filter and the rice distribution. *IEEE international ultrasonics symposium*. Vancouver, Canada, pp. 1694–1697.

Matte, P. (1986). Tectonics and plate tectonics model for the Variscan belt of Europe. *Tectonophysics*, *126*, 329–374.

Oggiano, G., & Di Pisa, A. (1992). Geologia della catena ercinica in Sardegna-Zona Assiale. In L. Carmignani, P. C. Pertusati, S. Barca, R. Carosi, A. Di Pisa, M. Gattiglio, C. Musumeci, & G. Oggiano (Eds.), *Struttura della Catena Ercinica in Sardegna. Gruppo Informale di Geologia Strutturale* (pp. 147–167). Siena: Centrooffset.

Pasci, S. (1997). Tertiary transcurrent tectonics of North-central Sardinia. *Bulletin de la Société Géologique de France*, *168*, 301–312.

Romero, J., Martìnez-Crego, B., Alcoverro, T., & Pérez, M. (2007). A multivariate index based on the seagrass *Posidonia oceanica* (POMI) to assess ecological status of coastal waters under the water framework directive (WFD). *Marine Pollution Bulletin*, *55*(1–6), 196–204. doi:10.1016/j.marpolbul.2006.08.032

Ruiz, J. M., & Romero, J. (2003). Effects of disturbances caused by coastal constructions on spatial structure, growth dynamics and photosynthesis of the seagrass *Posidonia oceanica*. *Marine Pollution Bulletin*, *46*(12), 1523–1533. doi:10.1016/j.marpolbul.2003.08.021